

# HDAC1 and HDAC2 control the transcriptional program of myelination and the survival of Schwann cells

Claire Jacob<sup>1</sup>, Carlos N Christen<sup>1,4</sup>, Jorge A Pereira<sup>1,4</sup>, Christian Somandin<sup>1,4</sup>, Arianna Baggiolini<sup>1</sup>, Pirmin Lötscher<sup>1</sup>, Murat Özçelik<sup>1</sup>, Nicolas Tricaud<sup>1</sup>, Dies Meijer<sup>2</sup>, Tepei Yamaguchi<sup>3</sup>, Patrick Matthias<sup>3</sup> & Ueli Suter<sup>1</sup>

**Histone deacetylases (HDACs) are major epigenetic regulators. We show that HDAC1 and HDAC2 functions are critical for myelination of the peripheral nervous system. Using mouse genetics, we have ablated *Hdac1* and *Hdac2* specifically in Schwann cells, resulting in massive Schwann cell loss and virtual absence of myelin in mutant sciatic nerves. Expression of *Sox10* and *Krox20*, the main transcriptional regulators of Schwann cell myelination, was greatly reduced. We demonstrate that in Schwann cells, HDAC1 and HDAC2 exert specific primary functions: HDAC2 activates the transcriptional program of myelination in synergy with *Sox10*, whereas HDAC1 controls Schwann cell survival by regulating the levels of active  $\beta$ -catenin.**

HDACs are chromatin-remodeling proteins. They exert epigenetic regulations by removing acetyl groups from histone tails, favoring condensed chromatin architecture that is less accessible for transcription factors. HDACs are commonly believed to act as transcriptional co-repressors<sup>1–3</sup> but they can also contribute to transcriptional activation<sup>4,5</sup>. In addition, HDACs act non-epigenetically by deacetylating non-histone targets<sup>6</sup>, including various transcription factors, implying that HDACs regulate transcriptional activity at different levels. HDACs are of particular interest to neurobiologists because HDAC inhibitors enhance neural regeneration<sup>7,8</sup> and control oligodendrocyte differentiation<sup>9–11</sup>. In contrast to oligodendrocytes in the CNS, Schwann cells, the myelination-competent cells of the peripheral nervous system (PNS), promote regeneration of damaged PNS and CNS axons and are contemplated in transplantation-based repair strategies after CNS injury<sup>12</sup>. In addition, Schwann cells are affected by common tumors<sup>13</sup> and in peripheral neuropathies<sup>14</sup>. Thus, a detailed understanding of Schwann cell biology is of major importance for uncovering their regenerative properties and developing efficient repair of damage to the CNS and PNS, and for treatment of peripheral nerve tumors and peripheral neuropathies.

Here we show that HDAC1 and HDAC2 are essential for Schwann cell myelination and survival: HDAC1 maintains Schwann cell survival by limiting the levels of active  $\beta$ -catenin (ABC), and HDAC2 is an inducer of the transcriptional program of myelination.

## RESULTS

### HDAC1 and HDAC2 control Schwann cell myelination and survival

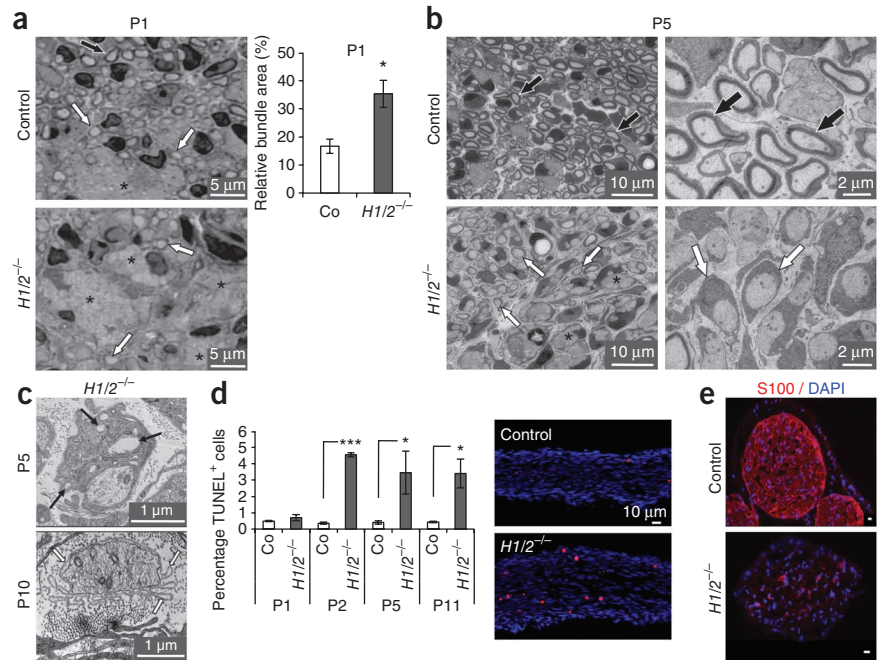
HDAC1 and HDAC2, coexpressed in Schwann cell nuclei (Supplementary Fig. 1a–d), were upregulated at postnatal day 1 (P1) and remained high until P5 in mouse sciatic nerves (referred

to as nerves hereafter; Supplementary Fig. 1e), suggesting postnatal functions of these proteins. To determine their functions, we depleted HDAC1 and/or HDAC2 in Schwann cells using *loxP*-flanked *Hdac1* and/or *Hdac2* alleles<sup>15</sup> and mice expressing the Cre recombinase under control of Desert Hedgehog gene regulatory elements (*Dhh<sup>Cre</sup>*). *Dhh<sup>Cre</sup>* is active in developing PNS glial cells, but not in neural crest cells or neurons<sup>16,17</sup>. *Dhh<sup>Cre</sup>Hdac1* or *Hdac2* homozygous knockout mice (*H1<sup>-/-</sup>* or *H2<sup>-/-</sup>*) were indistinguishable from their control littermates. HDAC1 and HDAC2 can compensate for each other in other systems<sup>11,18</sup>. Thus, we analyzed *Dhh<sup>Cre</sup>Hdac1-Hdac2* double homozygous knockout (*H1/2<sup>-/-</sup>*) mice.

*H1/2<sup>-/-</sup>* mice showed tremor and reduced hind limb mobility, and died around P17. Structural analyses revealed a partial axonal sorting delay at P1 (Fig. 1a). At P5, most axons in control mice (*Dhh<sup>Cre</sup>-*) were myelinated, whereas many *H1/2<sup>-/-</sup>* axons were sorted in a one-to-one relationship with Schwann cells but remained mostly unmyelinated (Fig. 1b). No myelin was found at P10 or P16 (data not shown and Supplementary Fig. 2a,b). At P5, many *H1/2<sup>-/-</sup>* Schwann cells showed signs of damage such as cytoplasm vacuolization and fragmentation, and at P10 empty basal lamina remnants were commonly found around axons (Fig. 1c). Massive apoptosis occurred in *H1/2<sup>-/-</sup>* nerves, with onset at P2 (Fig. 1d and Supplementary Table 1), resulting in virtual absence of Schwann cells at P16 (Fig. 1e and Supplementary Fig. 2a,b). Apoptotic cells were positive for the Schwann cell markers<sup>19</sup> GFAP, S100 (Supplementary Fig. 3a) and Oct-6 (Supplementary Fig. 3b). At P16, nerves were exclusively composed of aberrant mini-fascicles of axons (Supplementary Fig. 2a,b), surrounded by cells with perineurial-like characteristics such as prominent caveolae (data not shown) and expression of the tight junction proteins ZO-1 (ref. 20) and Claudin-1 that stain perineurial cells in control nerves (Supplementary Fig. 2c). In the absence of

<sup>1</sup>Institute of Cell Biology, Department of Biology, ETH Zurich, Zurich, Switzerland. <sup>2</sup>Department of Cell Biology and Genetics, Erasmus University Medical Center, Rotterdam, The Netherlands. <sup>3</sup>Friedrich Miescher Institute for Biomedical Research, Novartis Research Foundation, Basel, Switzerland. <sup>4</sup>These authors contributed equally to this work. Correspondence should be addressed to C.J. (claire.jacob@cell.biol.ethz.ch) or U.S. (usuter@cell.biol.ethz.ch).

**Figure 1** Partial axonal sorting delay, absence of myelination and massive Schwann cell loss in  $H1/2^{-/-}$  nerves. (**a-c**) Semithin (**a,b**) and ultrathin (**b,c**) sections of  $H1/2^{-/-}$  and  $Dhh^{Cre-}$  control nerves at P1, P5 and P10, and relative area covered by bundles (axon bundle area/total nerve area) quantified in P1 semithin sections of three control and three  $H1/2^{-/-}$  sciatic nerves. In **b**, images on the left were taken from semithin sections and images on the right from ultrathin sections. In **a,b**, white arrows highlight one-to-one relationships of axons with Schwann cells and black arrows point to myelinated axons in control nerves. Asterisks indicate axon bundles. In **c**, black arrows highlight Schwann cell cytoplasmic vacuoles and white arrows denote Schwann cell basal lamina remnants. (**d**) Percentage of TUNEL-positive cells in sections of P1, P2, P5 and P11  $H1/2^{-/-}$  and control (Co) nerves (three control and three  $H1/2^{-/-}$  mice per age group) and staining examples (TUNEL, red; DAPI, blue) at P2. (**e**) Immunofluorescence of S100 (red) on sections of P16  $H1/2^{-/-}$  and control nerves. Nuclei are labeled in blue with DAPI. S100 is a Schwann cell marker. Scale bars, 10  $\mu\text{m}$ . Two-tailed Student's  $t$ -test; \* $P < 0.05$ , \*\*\* $P < 0.001$ . Error bars, s.e.m.



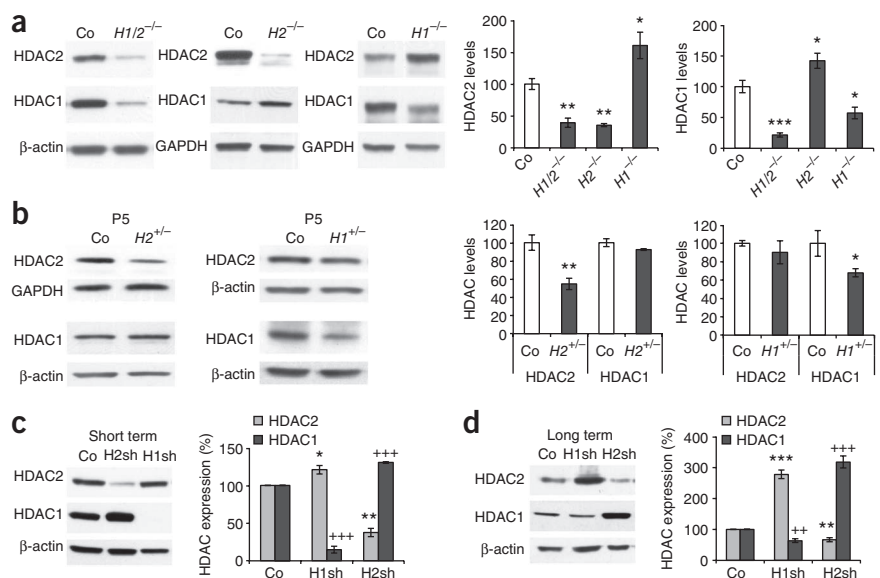
Schwann cells, perineurial cells seem to be able to support axonal survival, at least in the short term, as we found no signs of axonal degeneration in  $H1/2^{-/-}$  nerves up to P16, the latest time point examined. We conclude that the loss of HDAC1 and HDAC2 in Schwann cells results in severe hypomyelination and Schwann cell apoptosis.

### HDAC2 induces the Schwann cell myelination program

As expected from the genetic lesions, HDAC1 and HDAC2 were decreased in  $H1/2^{-/-}$  nerves (**Fig. 2** and **Supplementary Fig. 1b**). We then sought to identify the molecular mechanisms responsible for the severe hypomyelination caused by loss of HDAC1 and HDAC2. First, we examined known transcriptional regulators of

peripheral nerve myelination: Oct6, Sox10 and Krox20 (ref. 21). Western blot analysis of P5  $H1/2^{-/-}$  nerves revealed markedly reduced Sox10 and Krox20 levels while Oct6 was increased (**Fig. 3a** and **Supplementary Fig. 4a**). Increased Oct6 expression is likely secondary to reduced Krox20, as Krox20 is involved in Oct6 down-regulation at the promyelination stage<sup>22</sup>, but it might contribute to the observed phenotype because Oct6 overexpression causes hypomyelination<sup>23</sup>. Consistent with reduced Sox10 and Krox20, expression of the myelin proteins MAG, MBP and P0 was not detectable or barely detectable (**Fig. 3a** and **Supplementary Fig. 4a**). Further analyses revealed reduced Sox10, Krox20 and P0 from birth onwards (**Supplementary Fig. 5**). Taken together, our data indicate that

**Figure 2** In sciatic nerves and long term-transduced RSCs, loss of HDAC1 induces upregulation of HDAC2, and vice versa, whereas in  $H2^{+/-}$  or  $H1^{+/-}$  sciatic nerves and in short term-transduced cells, expression of the targeted HDAC is reduced without substantial upregulation of the untargeted HDAC. (**a-d**) Western blots of HDAC1 and HDAC2 in P5  $H1/2^{-/-}$ ,  $H2^{-/-}$ ,  $H1^{-/-}$  and  $Dhh^{Cre-}$  control (Co) nerves (**a**), in P5  $H2^{+/-}$ ,  $H1^{+/-}$  and control nerves (**b**), and in RSCs transduced for 3 d (**c**) or 2 weeks (**d**) with nontargeting control (Co),  $Hdac2$  (H2sh) or  $Hdac1$  (H1sh) shRNA lentiviruses. In **a,b**, graphs represent the ratio of HDAC1 or HDAC2 levels normalized to the loading control  $\beta$ -actin or GAPDH. This ratio has been multiplied by an arbitrary factor to set the control value to 100. In **c,d**, graphs represent the percentage of HDAC1 or HDAC2 levels (normalized to  $\beta$ -actin) compared to the control (set to 100%). Nerves of at least three control and three mutant mice were run and analyzed on the same gel, and each lane was loaded with one or two sciatic nerves from a single mouse (**a,b**). Three independent experiments were performed for each graph presented in **c,d**. Samples were run on the same gel but not always in consecutive lanes. Full-length blots are presented in **Supplementary Figure 10**. In **c,d**, significance is indicated by asterisks for HDAC2 and crosses for HDAC1. Two-tailed Student's  $t$ -test: \* $P < 0.05$ , \*\* $P < 0.01$ , \*\*\* $P < 0.001$ . Error bars, s.e.m.



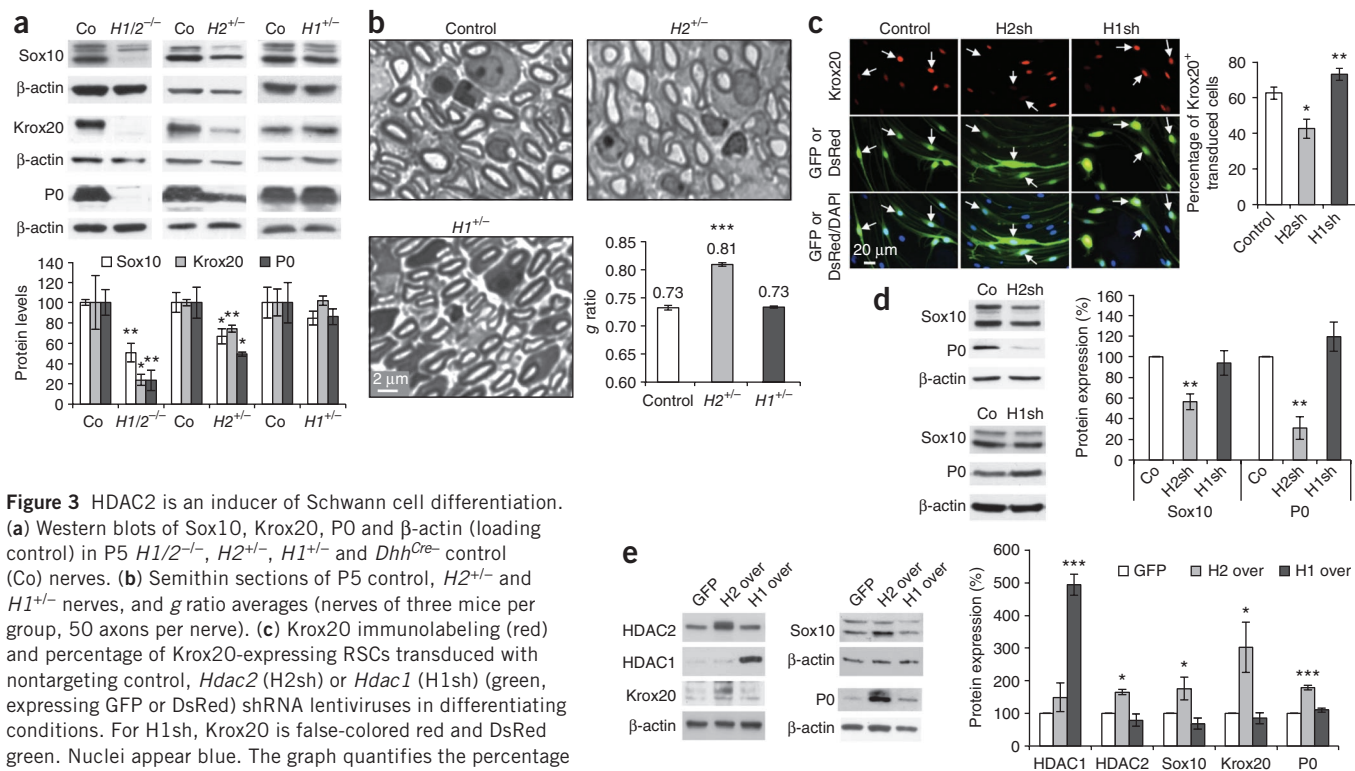


**Figure 3** HDAC2 is an inducer of Schwann cell differentiation.

(a) Western blots of Sox10, Krox20, P0 and  $\beta$ -actin (loading control) in P5  $H1/2^{-/-}$ ,  $H2^{+/-}$ ,  $H1^{+/-}$  and  $Dhh^{Cre}$  control (Co) nerves. (b) Semithin sections of P5 control,  $H2^{+/-}$  and  $H1^{+/-}$  nerves, and  $g$  ratio averages (nerves of three mice per group, 50 axons per nerve). (c) Krox20 immunolabeling (red) and percentage of Krox20-expressing RSCs transduced with nontargeting control,  $Hdac2$  (H2sh) or  $Hdac1$  (H1sh) (green, expressing GFP or DsRed) shRNA lentiviruses in differentiating conditions. For H1sh, Krox20 is false-colored red and DsRed green. Nuclei appear blue. The graph quantifies the percentage of cells expressing detectable Krox20, regardless of the expression level, and thus includes cells with reduced Krox20 expression. White arrows indicate transduced cells; at least 100 transduced cells counted per experiment (three independent experiments). (d) Western blots of Sox10, P0 and  $\beta$ -actin in RSCs transduced with nontargeting control (Co), H2sh or H1sh lentiviruses. (e) Western blots of HDAC2, HDAC1, Krox20, Sox10, P0 and  $\beta$ -actin in differentiated RSCs transfected with GFP (control), HDAC2 (H2 over) or HDAC1 (H1 over) overexpressing constructs. In **a,d**, samples were run on the same gel but not always in consecutive lanes. In **a**, the graph represents the ratio of the proteins normalized to  $\beta$ -actin (ratio multiplied by an arbitrary factor to set the control to 100; at least three nerves of different mice per group). In **d,e**, graphs represent quantification compared to control (set equal to 100%) of three independent experiments. Two-tailed Student's  $t$ -test; \* $P < 0.05$ , \*\* $P < 0.01$ , \*\*\* $P < 0.001$ . Error bars, s.e.m. Full-length blots are presented in **Supplementary Figure 10**.

reduced expression of myelination inducers and myelin proteins contributes to the hypomyelination in P5  $H1/2^{-/-}$  nerves.

To identify potential defects resulting from the loss of a single HDAC, we analyzed P5  $H1^{-/-}$  and  $H2^{-/-}$  and  $Dhh^{Cre}$  single  $Hdac1$  or  $Hdac2$  heterozygous ( $H1^{+/-}$  or  $H2^{+/-}$ ) nerves. In  $H1^{-/-}$  and  $H2^{-/-}$  nerves, the targeted HDAC was decreased, but the untargeted HDAC was upregulated (**Fig. 2a**). No alteration of Sox10, Krox20 and myelin proteins was detectable (**Supplementary Fig. 6**), indicating compensatory mechanisms between the two HDACs. Of note, in P5  $H1^{+/-}$  and  $H2^{+/-}$  nerves, the targeted HDAC was decreased and no upregulation of the untargeted HDAC occurred (**Fig. 2b**).  $H2^{+/-}$  nerves showed reduced Sox10, Krox20 and myelin proteins (**Fig. 3a** and **Supplementary Fig. 4a**) and increased  $g$  ratios (axon diameter / (axon + myelin diameter)) of myelinated axons, whereas we found no such alterations in  $H1^{+/-}$  (**Fig. 3b**),  $H1^{-/-}$  or  $H2^{-/-}$  nerves (data not shown). These findings identified HDAC2 as a regulator of myelination.

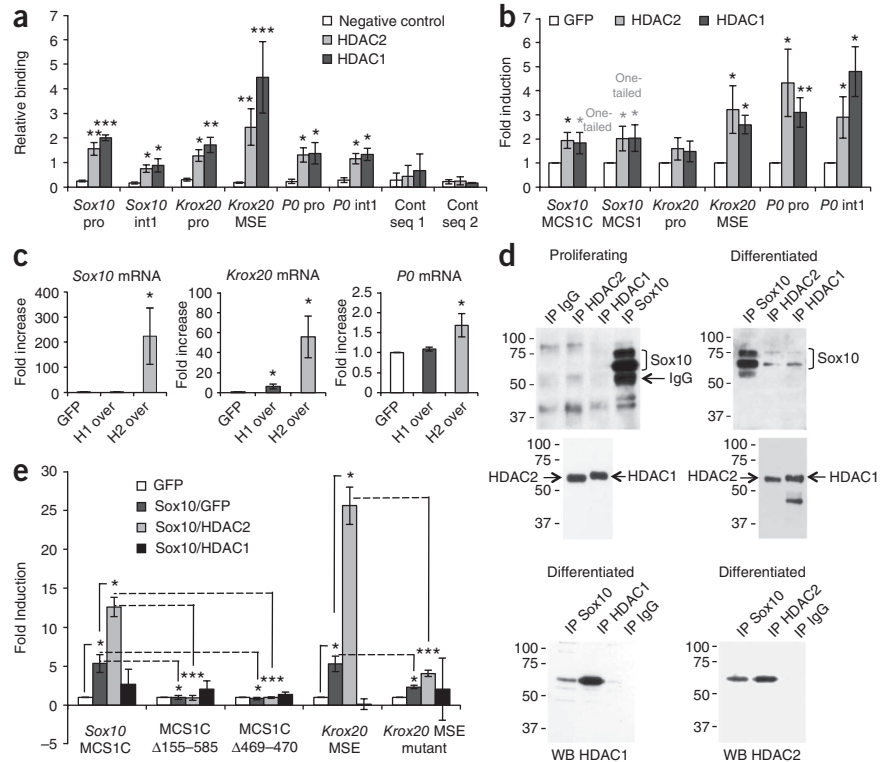
Complementary *in vitro* experiments using acute (short-term, with minimal upregulation of the untargeted HDAC; **Fig. 2c**) but not prolonged (long-term, with pronounced upregulation of the untargeted HDAC; **Fig. 2d**) downregulation of HDAC1 or HDAC2 by specific short hairpin RNA (shRNA) in primary rat Schwann cells (RSCs) corroborated these results. Downregulation of HDAC2, but not HDAC1, resulted in decreased Sox10, Krox20, P0 and MAG (**Fig. 3c,d** and **Supplementary Fig. 4b**). Conversely, overexpression of HDAC2, but not HDAC1, increased Sox10, Krox20 and P0 (**Fig. 3e**) under differentiating conditions.

### HDAC2 acts in synergy with Sox10

We next investigated the molecular mechanisms by which HDAC1 and HDAC2 regulate Schwann cell myelination. HDACs modify transcription. Thus, we performed comparative transcriptome microarray analyses of  $H1/2^{-/-}$  nerves versus control littermates at P2 (**Supplementary Table 1**). As expected, we found severely reduced  $Krox20$  ( $Egr2$ ) mRNA levels and a trend toward decreased  $Sox10$  mRNA. Increased myelin inhibitor expression could cause hypomyelination<sup>24</sup>, and HDACs regulate the expression of inhibitors of myelination in oligodendrocytes<sup>10</sup>. In  $H1/2^{-/-}$  nerves, however,  $Id2$  mRNA was reduced,  $Pax3$ ,  $Hes1$  and  $Hes5$  not affected, and  $Sox2$ ,  $Jun$  and  $Notch1$  only slightly increased (**Supplementary Table 1**). We confirmed reduced  $Id2$  protein levels in P5  $H1/2^{-/-}$  nerves; c-Jun and Sox2 were not detectably changed (**Supplementary Fig. 7a**). Schwann cell proliferation, usually correlating with myelination inhibitor expression<sup>24</sup>, was not significantly altered in P2  $H1/2^{-/-}$  nerves (**Supplementary Fig. 7b**) or in RSCs transduced with  $Hdac2$  or  $Hdac1$  shRNA (**Supplementary Fig. 7c**). We conclude that upregulation of myelination inhibitors is unlikely to account for the observed hypomyelination.

Next, we asked whether HDAC1 and/or HDAC2 regulate  $Sox10$ ,  $Egr2$  ( $Krox20$ ) and/or  $Mpz$  ( $P0$ ) transcription. Using chromatin immunoprecipitation in RSCs, we found both HDAC1 and HDAC2 bound to the  $Sox10$  promoter and intron 1, the  $Krox20$  promoter and  $Krox20$  MSE (myelinating Schwann cell element<sup>25</sup> controlling  $Krox20$  expression in Schwann cells after birth), and the  $P0$  promoter and

**Figure 4** Transcriptional regulation of the myelination program by HDACs. **(a)** Relative binding of antibodies specific for HDAC2 (anti-HDAC2), anti-HDAC1 or rabbit IgG (negative control) to *Sox10* promoter (pro), *Sox10* intron 1 (int1), *Krox20* pro, *Krox20* MSE, *P0* pro, *P0* int1, control sequence (Cont seq) 1 or Cont seq 2, compared to histone H3 (HH3) antibody (positive control, set equal to 1). **(b)** Luciferase fold induction of *Sox10* MCS1C, *Sox10* MCS1, *Krox20* pro, *Krox20* MSE, *P0* pro and *P0* int1 constructs by HDAC2 or HDAC1 overexpression, compared to that seen with GFP expression (set equal to 1), in differentiated RSCs. **(c)** *Sox10*, *Krox20* and *P0* mRNA fold induction, normalized to *Gapdh*, in RSCs overexpressing HDAC1 (H1 over) or HDAC2 (H2 over), compared to that in RSCs expressing GFP (set equal to 1). **(d)** Immunoprecipitation (IP) of HDAC2, HDAC1, *Sox10* or negative control IP (IgG) in proliferating or differentiated RSCs, and western blot (WB) analysis of *Sox10*, HDAC2 and HDAC1. For reblots of HDAC1 and HDAC2, the membranes were sliced to incubate each IP with the corresponding antibody. **(e)** Luciferase fold induction of *Sox10* MCS1C, *Sox10* MCS1C mutants  $\Delta 155-585$  and  $\Delta 469-470$ , *Krox20* MSE and *Krox20* MSE mutant constructs by double overexpression of *Sox10*/GFP, *Sox10*/HDAC2 or *Sox10*/HDAC1, compared to that seen with GFP expression, in differentiated RSCs. At least three independent experiments per graph or IP. Two-tailed Student's *t*-test, unless stated otherwise in the figure; \**P* < 0.05, \*\**P* < 0.01, \*\*\**P* < 0.001. Error bars, s.e.m. Full-length blots are presented in **Supplementary Figure 10**.



intron 1 (Fig. 4a). Exogenous DNA transiently introduced to cells is packaged into nucleosomes to about the same degree as endogenous DNA<sup>26</sup>. Thus, we overexpressed HDAC1 or HDAC2 in RSCs and determined, by luciferase gene reporter assays, whether HDAC1 and

HDAC2 also activate regulatory regions of the *Sox10*, *Krox20* and *P0* genes. Both HDAC1 and HDAC2 activated the *Sox10* MCS1C and MCS1 regulatory elements (containing the promoter and intron 1 region, respectively), *Krox20* MSE, and *P0* promoter and intron 1, but

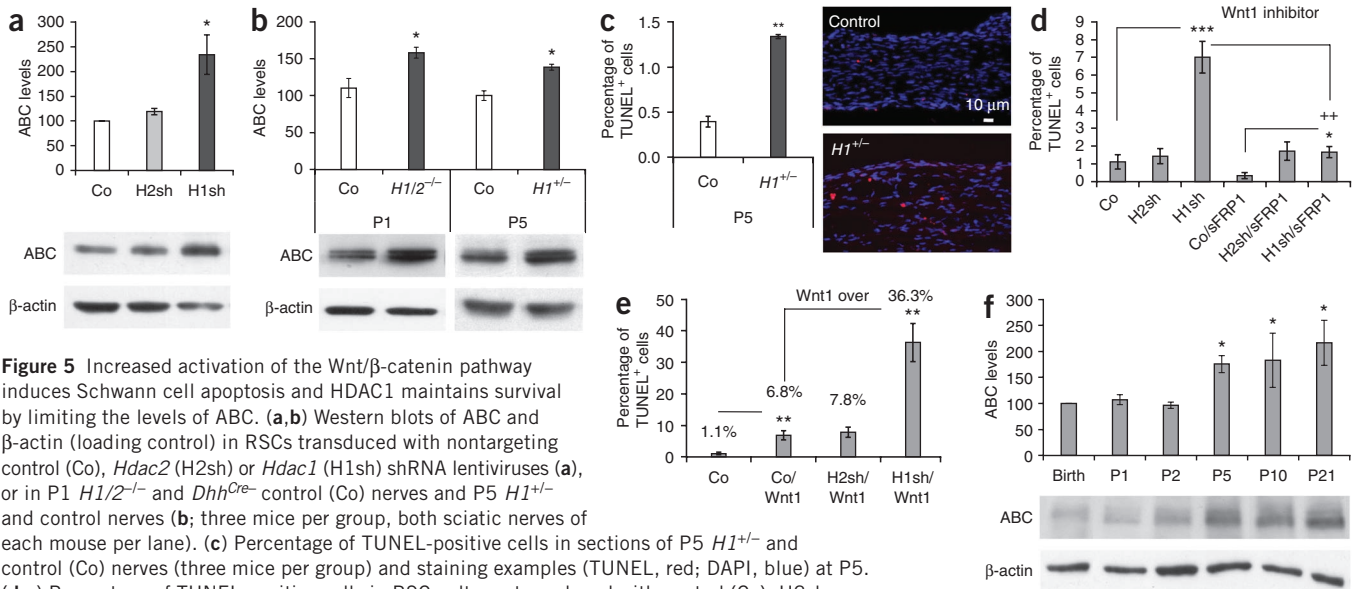


**Figure 5** Increased activation of the Wnt/ $\beta$ -catenin pathway induces Schwann cell apoptosis and HDAC1 maintains survival by limiting the levels of ABC. **(a,b)** Western blots of ABC and  $\beta$ -actin (loading control) in RSCs transduced with nontargeting control (Co), *Hdac2* (H2sh) or *Hdac1* (H1sh) shRNA lentiviruses (**a**), or in P1 *H1/2*<sup>-/-</sup> and *Dhh*<sup>Cre</sup>- control (Co) nerves and P5 *H1*<sup>+/-</sup> and control nerves (**b**); three mice per group, both sciatic nerves of each mouse per lane). **(c)** Percentage of TUNEL-positive cells in sections of P5 *H1*<sup>+/-</sup> and control (Co) nerves (three mice per group) and staining examples (TUNEL, red; DAPI, blue) at P5. **(d,e)** Percentage of TUNEL-positive cells in RSC cultures transduced with control (Co), H2sh or H1sh lentiviruses, treated or not with sFRP1 (**d**), or co-transduced with Wnt1-overexpression (over) lentiviruses (**e**). **(f)** Western blots of ABC and  $\beta$ -actin in control nerves at birth, P1, P2, P5, P10 and P21 (three sets of two to four mice per age group). In **a,b,f**, graphs represent ABC levels normalized to  $\beta$ -actin (**a**, Co set equal to 100%; **b**, for P1 Co and *H1/2*<sup>-/-</sup>, percentages calculated compared to ABC in control nerves, and for P5 Co and *H1*<sup>+/-</sup>, ratios multiplied by an arbitrary factor to set the control to 100; **f**, birth level set equal to 100%). In **d,e**, at least three independent experiments were carried out. Error bars, s.e.m. Two-tailed Student's *t*-test; \**P* < 0.05, \*\**P* or \*\*\**P* < 0.01, \*\*\**P* < 0.001. In **b**, samples were run on the same gel but not always in consecutive lanes. Full-length blots are presented in **Supplementary Figure 10**.

not the *Krox20* promoter (Fig. 4b). To determine whether these activations resulted in more transcripts, we performed quantitative RT-PCR analyses. HDAC2 overexpression markedly increased *Sox10* and *Krox20* mRNAs and slightly increased *P0* mRNA, whereas HDAC1 overexpression only minimally increased *Krox20* mRNA (Fig. 4c). This indicates that HDAC1, despite its ability to bind to and activate regulatory regions of *Sox10*, *Krox20* and *P0* genes, is not able to induce the production of the corresponding mRNAs, or is less efficient than HDAC2 at doing so.

HDACs have not been shown to bind DNA directly. Thus, we searched for binding partners that may allow binding of HDAC1 and/or HDAC2 to regions of *Sox10*, *Krox20* and *P0* that they activate. Sox10 autoactivates its own transcription by binding to elements located upstream of the transcription start site<sup>27</sup>. Sox10 also binds to and activates the *Krox20* MSE, as well as the *P0* promoter and intron 1 (ref. 28). Oct6 can bind to the *Krox20* MSE and activate *Krox20* transcription<sup>28</sup>. Thus, we asked whether HDAC1 and HDAC2 interact with Sox10 and/or Oct6. Using coimmunoprecipitation in RSCs, we found that both HDAC1 and HDAC2 interacted with Sox10 under differentiating, but not proliferating, conditions (Fig. 4d). No coimmunoprecipitation of HDAC1 or HDAC2 was detected with Oct6 (data not shown). In luciferase gene reporter assays, Sox10 overexpression significantly activated the *Sox10* MCS1C and *Krox20* MSE regions, and only co-overexpression of HDAC2, but not of HDAC1, with Sox10 resulted

in synergistic activation (Fig. 4e). When Sox10 was overexpressed alone or together with HDAC1 or HDAC2, we found no or minimal activation of *Sox10* MCS1C and *Krox20* MSE mutants having their Sox10 binding sites deleted or mutated (Fig. 4e). Taken together, these data indicate that HDAC2 activates *Sox10* and *Krox20* transcription by interacting with Sox10.

### HDAC1 maintains survival by limiting the levels of ABC

Next, we searched for potential specific functions of HDAC1 in Schwann cells. We found that knocking down HDAC1 in RSCs resulted in increased ABC, whereas HDAC2 knockdown had no such effect (Fig. 5a). Consistent with these findings, ABC was increased *in vivo* at P5 in *H1<sup>+/-</sup>* nerves, and it was already increased at P1 in *H1/2<sup>-/-</sup>* nerves (Fig. 5b), though not at P1 in *H1<sup>+/-</sup>* nerves (data not shown). No ABC increase was detectable in *H2<sup>+/-</sup>*, *H1<sup>-/-</sup>* or *H2<sup>-/-</sup>* nerves (data not shown). This caught our interest because HDAC inhibitors induce carcinoma cell apoptosis through an increase in ABC<sup>29</sup>, and we had observed a sharp increase of apoptosis in *H1/2<sup>-/-</sup>* nerves compared to controls starting at P2 (Fig. 1d and Supplementary Table 1). To determine whether increased ABC at P5 in *H1<sup>+/-</sup>* nerves also correlated with increased apoptosis, we analyzed *H1<sup>+/-</sup>* nerves at P2 and P5. We found increased apoptosis at P5 (Fig. 5c) but not at P2 (data not shown). Apoptosis was not altered in *H2<sup>+/-</sup>*, *H1<sup>-/-</sup>* or *H2<sup>-/-</sup>* nerves at P2 or P5 (data not shown). On the basis of these data,

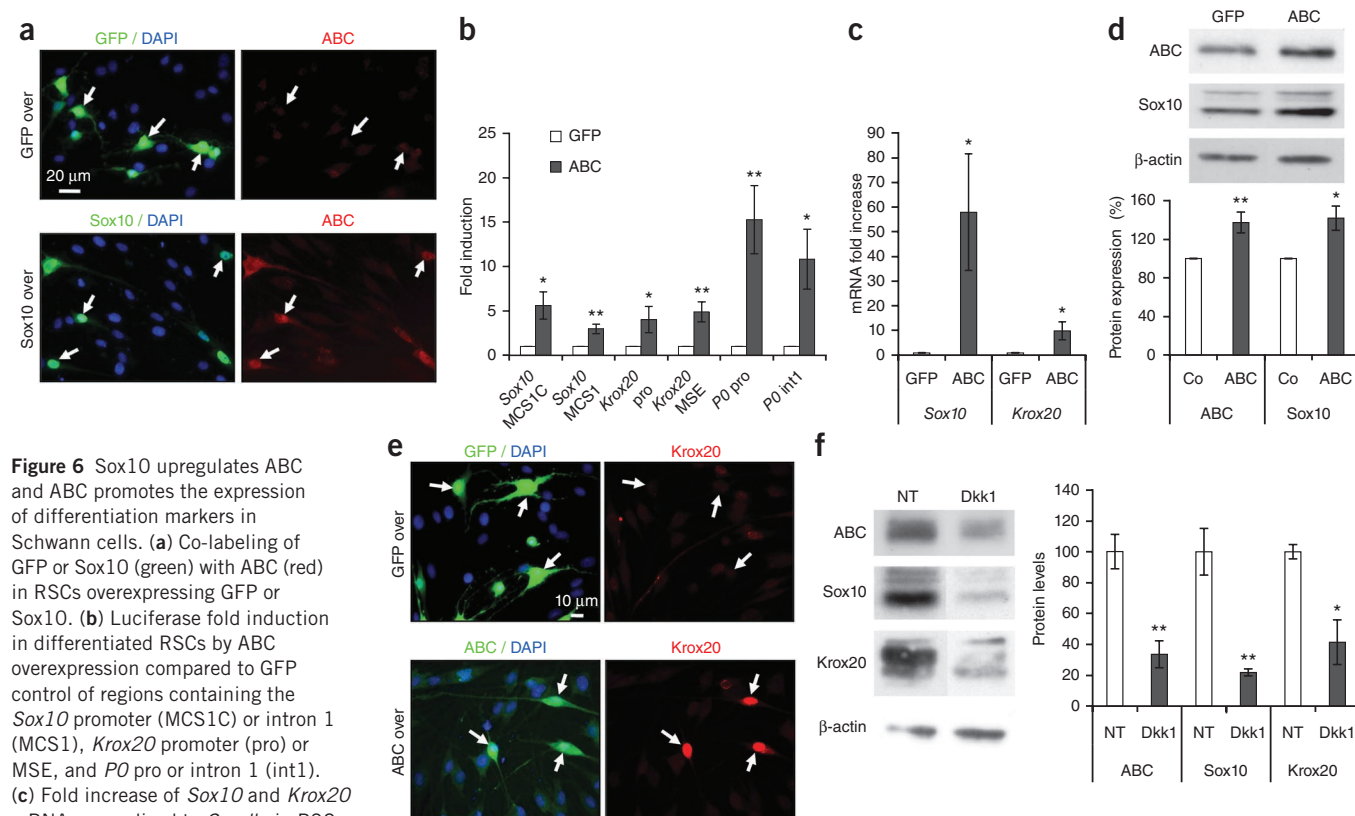


**Figure 6** Sox10 upregulates ABC and ABC promotes the expression of differentiation markers in Schwann cells. **(a)** Co-labeling of GFP or Sox10 (green) with ABC (red) in RSCs overexpressing GFP or Sox10. **(b)** Luciferase fold induction in differentiated RSCs by ABC overexpression compared to GFP control of regions containing the *Sox10* promoter (MCS1C) or intron 1 (MCS1), *Krox20* promoter (pro) or MSE, and *P0* pro or intron 1 (int1). **(c)** Fold increase of *Sox10* and *Krox20* mRNA, normalized to *Gapdh*, in RSCs overexpressing ABC compared to GFP (set equal to 1). **(d)** ABC, Sox10 and  $\beta$ -actin (loading control) western blots in RSCs overexpressing GFP or ABC and quantification (normalized to  $\beta$ -actin) compared to GFP control (set equal to 100%). **(e)** Co-labeling of GFP or ABC (green) and *Krox20* (red) in differentiated RSCs overexpressing (over) GFP or ABC. **(f)** ABC, Sox10, *Krox20* and  $\beta$ -actin western blots in control mouse sciatic nerves treated with Dkkopf-1 (Dkk1) or not treated (NT), and graph representing the ratio of the proteins normalized to  $\beta$ -actin. This ratio has been multiplied by an arbitrary factor to set the control to 100. Sciatic nerves of at least three NT and three Dkk1 mice were used (one sciatic nerve of a single mouse per lane). In **a,e**, at least three immunostainings were done and at least 100 cells were analyzed in each case per experiment; white arrows represent some overexpressing cells; nuclei are labeled in blue with DAPI (see text). In **b-d**, at least three independent experiments were carried out. Error bars, s.e.m. Two-tailed Student's *t*-test; \* $P < 0.05$ , \*\* $P < 0.01$ . In **d,f**, samples were run on the same gel but not in consecutive lanes. Full-length blots are presented in **Supplementary Figure 10**.

we hypothesized that the HDAC1-ABC connection regulates Schwann cell survival. Indeed, knocking down HDAC1, but not HDAC2, resulted in increased apoptosis of RSCs. This effect was largely prevented by the Wnt1 inhibitor sFRP1 (secreted frizzled-related protein 1) (Fig. 5d). Furthermore, Wnt1 overexpression induced Schwann cell apoptosis, which was synergistically increased by HDAC1 down-regulation (Fig. 5e). Similarly, overexpression of constitutively active  $\beta$ -catenin resulted in massive apoptosis: all ABC-overexpressing Schwann cells were either dead or TUNEL-positive 3 d after transfection (data not shown).

Additionally, and consistent with previous findings in oligodendrocytes<sup>11</sup>, ABC co-immunoprecipitated with the transcription factor Tcf-4 in RSCs. Overexpression of HDAC1, but not of HDAC2, decreased this interaction (Supplementary Fig. 8). Taken together, our data indicate that HDAC1 regulates Schwann cell survival and that loss of HDAC1 induces Schwann cell apoptosis through increases in ABC. Of note, quantification of ABC during development in postnatal mouse nerves revealed that ABC was maintained at steady state from birth until at least P2. At P5, ABC was increased and remained high until at least P21 (Fig. 5f). These findings suggest that limitation of ABC by HDAC1 in Schwann cells is critical within the first postnatal days but not in later development.

#### Sox10 regulates ABC, promoting differentiation of Schwann cells

Because ABC levels were dynamically regulated in mouse nerves, we examined the potential function of ABC in Schwann cell differentiation. We found that Sox10 overexpression resulted in robust upregulation of ABC in RSCs. All Sox10-overexpressing cells also expressed levels of ABC above a fixed arbitrary threshold, while none of the GFP-expressing cells showed ABC levels above threshold (Fig. 6a). Furthermore, ABC overexpression rapidly induced the activation of promoters and regulatory regions of *Sox10*, *Krox20* and *P0* in RSCs (Fig. 6b) and increased Sox10 and Krox20 expression at mRNA (Fig. 6c) and protein levels (Fig. 6d,e). Upregulation of Krox20 by overexpressed ABC was robust and consistent, as all cells overexpressing ABC showed Krox20 expression higher than a fixed arbitrary expression threshold, whereas none of the GFP-expressing cells showed Krox20 above threshold. These findings indicate that ABC can promote Schwann cell differentiation.

To further assess the relevance of ABC function in Schwann cells, we used an acute *in vivo* pharmacological approach. We reduced ABC levels by administering Dickkopf-1 (Dkk1, an inhibitor of the Wnt canonical pathway) to mice at birth and collected their nerves at P2. Dkk1 strongly decreased ABC, Sox10 and Krox20 expression (Fig. 6f), without apparent toxicity or changes in apoptosis (data not shown), supporting our findings that the Wnt/ $\beta$ -catenin pathway contributes to PNS myelination.

#### DISCUSSION

We have found that HDAC1 and HDAC2 are essential for Schwann cell myelination and survival after birth. Myelination is primarily promoted by HDAC2 through transcriptional regulation of myelination-related gene expression. Cell survival is primarily controlled by HDAC1 in connection with ABC regulation, and ABC also functions in differentiation. In Schwann cells, HDAC1 and HDAC2 can efficiently compensate for the loss of each other under special circumstances owing to dynamic compensation mechanisms. However, we were able to dissect the distinct functions of HDAC1 and HDAC2 in *H1*<sup>+/-</sup> and *H2*<sup>+/-</sup> mice in combination with complementary *in vitro* approaches.

#### Severe hypomyelination and apoptosis in *H1/2*<sup>-/-</sup> nerves

The deletion of both HDACs in Schwann cells resulted in partial axonal sorting defects. However, many axons were successfully sorted at P5 and expressed high levels of Oct6, but myelination was blocked. This is likely due to reduced expression of the main transcriptional regulators controlling these events, Sox10 and Krox20. Consequently, myelin protein expression was also low. In contrast to findings in Schwann cell-specific Sox10-deficient mice<sup>30</sup>, loss of HDAC1 and HDAC2 allowed Schwann cells to progress beyond the immature stage to promyelination. This may be due to residual Sox10 expression in *H1/2*<sup>-/-</sup> nerves, or other unknown mechanisms that may relate to the maintained expression of Oct6, as Oct6 was not expressed in *Sox10*<sup>-/-</sup> nerves<sup>30</sup>. Markedly reduced Krox20 expression is in line with the arrest of Schwann cells at the promyelinating stage in *H1/2*<sup>-/-</sup> nerves, as this phenocopies effects of loss of Krox20 in Schwann cells<sup>25,31</sup>.

Loss of HDAC1 and HDAC2 in Schwann cells resulted in increased apoptosis with onset at P2. This increase was massive, and at P16 (the end stage analyzed), no more Schwann cells or endoneurial fibroblasts were detectable in *H1/2*<sup>-/-</sup> nerves. Instead, cells with perineurial-like characteristics were present in the endoneurium and had surrounded mini-fascicles of naked axons. A similar phenomenon has been described in *Dhh* knockout nerves<sup>20</sup>, but *Dhh* levels were not changed in *H1/2*<sup>-/-</sup> nerves (data not shown). We cannot exclude the possibility that loss of HDAC1 and HDAC2 in Schwann cells produced a fate switch into perineurial-like cells. However, we favor the interpretation that perineurial cells have invaded *H1/2*<sup>-/-</sup> nerves owing to Schwann cell loss, as Schwann cells in *H1/2*<sup>-/-</sup> nerves showed signs of damage accompanied by massively increased apoptosis.

#### HDAC2, but not HDAC1, primarily induces myelination

HDAC1 and HDAC2 were upregulated in P1 nerves, remained high during early postnatal development, and decreased progressively until adulthood. This regulation suggests that HDAC1 and HDAC2 might have important functions during early postnatal PNS development.

We found that both HDACs bound to and activated regulatory regions of *Sox10*, *Krox20* and *P0*, and that they both associated with Sox10 in Schwann cells upon induction of differentiation. However, only HDAC2 expression increased the levels of Schwann cell differentiation markers. Sox10 is key in this critical regulatory mechanism by activating its own transcription and the transcription of *Krox20* in synergy with HDAC2, but not with HDAC1. Consistent with this regulatory function of HDAC2, we observed reduced myelin sheath thickness in early postnatal *H2*<sup>+/-</sup> but not *H1*<sup>+/-</sup> nerves. We conclude that primarily HDAC2, but not HDAC1, is an inducer of the transcriptional program of Schwann cell myelination.

#### HDAC1 maintains Schwann cell survival by limiting ABC

In contrast to findings in double mutants of *Hdac1* and *Hdac2* in oligodendrocyte precursors<sup>11</sup>, but in accordance with studies of double mutants in other systems<sup>15,18</sup>, we found strongly increased Schwann cell apoptosis. Onset in *H1/2*<sup>-/-</sup> nerves was at P2 and correlated with increased ABC. In *H1*<sup>+/-</sup> nerves, but not in *H2*<sup>+/-</sup> nerves, increased apoptosis also occurred, but with onset at P5, again correlated with increased ABC. In RSCs, knockdown of HDAC1, but not of HDAC2, resulted in increased ABC and increased apoptosis. This effect was largely rescued by a Wnt1 inhibitor and synergistically enhanced by concomitant Wnt1 overexpression. Thus, we conclude that during early postnatal Schwann cell development, HDAC1 maintains survival by limiting ABC.



In RSCs, Sox10 overexpression induced a marked increase of ABC, and ABC initially promoted Schwann cell differentiation before causing apoptosis. Removal of HDAC1 did not affect myelination but resulted in increased ABC. We interpret these findings to mean that HDAC1 may not primarily promote differentiation because the primary function of HDAC1 is to limit the levels of ABC, which also limits ABC-induced Schwann cell differentiation. ABC was expressed at steady-state levels in mouse nerves from birth till at least P2, and at P5 increased and remained high until at least P21. It seems likely that ABC is increased by Sox10 to enhance the myelination process. However, the molecular mechanisms by which ABC induces Schwann cell differentiation remain to be identified. The active form of  $\beta$ -catenin translocates to the nucleus and associates with a member of the TCF/LEF1 family of transcription factors to activate a specific set of downstream genes<sup>32</sup>. A potential mechanism by which ABC could increase differentiation is direct regulation of Sox10 transcription, as several potential binding sites for LEF1 are present in the *Sox10* gene<sup>27,33</sup>. Moreover, overexpression of ABC in neural crest cells can induce ectopic expression of Sox10 (ref. 33). ABC may also activate *Krox20* transcription by a direct mechanism, not only through Sox10 upregulation, because we found that overexpression of ABC could activate both the *Krox20* promoter and *Krox20* MSE, whereas Sox10 activates the *Krox20* MSE but not the *Krox20* promoter (ref. 21 and data not shown).

We note that in a related study<sup>34</sup>, activation of Wnt signaling by  $\beta$ -catenin stabilization did not affect Schwann cell myelination. The reasons for this difference are not clear.

#### HDAC1/2 levels in Schwann cells are dynamic and interdependent

An unexpected result in our study is the finding that single HDAC heterozygous nerves showed a detectable phenotype, whereas single HDAC homozygous knockout nerves did not. This indicates compensatory mechanisms in single HDAC homozygous but not in single heterozygous knockout nerves. These compensatory mechanisms appear to occur, at least partly, through upregulation of HDAC1 when HDAC2 is absent, and vice versa. The compensation seems to be time dependent, as long-term downregulation of one HDAC resulted in strong upregulation of the other HDAC, whereas short-term downregulation induced only a minimal increase. Other HDACs may also participate in the compensation, but we did not detect increases of HDAC3 or HDAC8 (data not shown), the other class I HDAC members.

In single heterozygous nerves, there was no upregulation of the untargeted HDAC, suggesting that upregulation of the untargeted HDAC is induced only when the targeted HDAC is expressed below a threshold level. In single heterozygous nerves, the targeted HDAC was only transiently reduced (data not shown), and, consistent with this, we found only transient hypomyelination and increased apoptosis in *H2<sup>+/-</sup>* and *H1<sup>+/-</sup>* nerves, respectively. This indicates that Schwann cells, when possible, preferentially increase expression of the partially missing HDAC species, rather than upregulating the untargeted HDAC. This is in line with the hypothesis that HDAC1 is more efficient than HDAC2 at fulfilling its primary functions, and vice versa. As a result, when one HDAC is completely lacking, the remaining HDAC may need to be substantially upregulated to efficiently compensate for the missing HDAC. Thus, the expression of HDAC1 and HDAC2 in Schwann cells is dynamic and can be appropriately adjusted depending on the need and the availability of HDAC1 and HDAC2 in the cell. Regardless of the molecular basis for these observations, our findings emphasize that when proteins with HDAC-like general functions are analyzed in transgenic

mice, heterozygous nulls should be examined, even when no alterations are detected in homozygous nulls.

#### Conclusion

HDAC1 and HDAC2 are essential for myelination of the PNS and Schwann cell survival (**Supplementary Fig. 9**). Although both HDACs can compensate for the loss of the other if one of them is fully removed, they have distinct specific main functions under normal physiological conditions: HDAC2 is a principal inducer of differentiation, whereas HDAC1 regulates survival. HDACs are commonly thought to act through transcriptional repression. We demonstrate, in line with other recent studies<sup>4,5</sup>, that HDACs also cause transcriptional activation. Additionally, we provide mechanistic understandings of how HDACs activate transcription in Schwann cells and identify their functions in these cells during postnatal PNS development. This knowledge is important for our understanding of basic nerve biology and potential medical application and will also help unravel the functions of HDACs in other cellular systems.

#### METHODS

Methods and any associated references are available in the online version of the paper at <http://www.nature.com/natureneuroscience/>.

**Accession codes.** Gene Expression Omnibus: Microarray data have been deposited with accession code GSE27451.

*Note: Supplementary information is available on the Nature Neuroscience website.*

#### ACKNOWLEDGMENTS

We thank M. Wegner (Universität Erlangen-Nürnberg), E. Seto (Moffitt Cancer Center), S. Schreiber (Harvard University), Z. Werb and B. Welm (University of Utah), J. Crabtree (Stanford University), T. Reya (Duke University Medical Center), W.J. Pavan (US National Institutes of Health), A. McCallion and M. Prasad (Johns Hopkins University School of Medicine) and D.R. Colman (McGill University) for providing constructs and antibodies, T. Meier, W. Seufert and N. Mantei for critically reading the manuscript and the Functional Genomic Center Zurich for gene array analyses. These studies were supported by two Swiss National Science Foundation (SNSF) grants, a Marie-Heim Vögtlin subsidy (PMPDP3\_122738/1) to C. Jacob, and another SNSF grant to U. Suter, and by a grant from the Swiss National Center for Competence in Research (NCCR) Neural Plasticity and Repair to U. Suter. The work in the laboratory of P. Matthias was supported by the Novartis Research Foundation.

#### AUTHOR CONTRIBUTIONS

C.J. designed the study, analyzed the data and wrote the manuscript; C.J., C.N.C., J.A.P., C.S., A.B., P.L., M.O. and N.T. performed and analyzed the experiments; D.M., T.Y. and P.M. generated and provided crucial mouse lines and support; U.S. conceived and supervised the study and co-wrote the manuscript. All authors commented on the manuscript.

#### COMPETING FINANCIAL INTERESTS

The authors declare no competing financial interests.

Published online at <http://www.nature.com/natureneuroscience/>.

Reprints and permissions information is available online at <http://npg.nature.com/reprintsandpermissions/>.

1. Kadosh, D. & Struhl, K. Repression by Ume6 involves recruitment of a complex containing Sin3 corepressor and Rpd3 histone deacetylase to target promoters. *Cell* **89**, 365–371 (1997).
2. Rundlett, S.E., Carmen, A.A., Suka, N., Turner, B.M. & Grunstein, M. Transcriptional repression by UME6 involves deacetylation of lysine 5 of histone H4 by RPD3. *Nature* **392**, 831–835 (1998).
3. Taunton, J., Hassig, C.A. & Schreiber, S.L. A mammalian histone deacetylase related to the yeast transcriptional regulator Rpd3p. *Science* **272**, 408–411 (1996).
4. Zupkowitz, G. *et al.* Negative and positive regulation of gene expression by mouse histone deacetylase 1. *Mol. Cell. Biol.* **26**, 7913–7928 (2006).
5. Wang, Z. *et al.* Genome-wide mapping of HATs and HDACs reveals distinct function in active and inactive genes. *Cell* **138**, 1019–1031 (2009).
6. Glozak, M.A., Sengupta, N., Zhang, X. & Seto, E. Acetylation and deacetylation of non-histone proteins. *Gene* **363**, 15–23 (2005).

7. Kazantsev, A.G. & Thompson, L.M. Therapeutic application of histone deacetylase inhibitors for central nervous system disorders. *Nat. Rev. Drug Discov.* **7**, 854–868 (2008).
8. Chuang, D.M., Leng, Y., Marinova, Z., Kim, H.J. & Chiu, C.T. Multiple roles of HDAC inhibition in neurodegenerative conditions. *Trends Neurosci.* **32**, 591–601 (2009).
9. Shen, S., Li, J. & Casaccia-Bonnel, P. Histone modifications affect timing of oligodendrocyte progenitor differentiation in the developing rat brain. *J. Cell Biol.* **169**, 577–589 (2005).
10. Shen, S. *et al.* Age-dependent epigenetic control of differentiation inhibitors is critical for remyelination efficiency. *Nat. Neurosci.* **11**, 1024–1034 (2008).
11. Ye, F. *et al.* HDAC1 and HDAC2 regulate oligodendrocyte differentiation by disrupting the  $\beta$ -catenin–TCF interaction. *Nat. Neurosci.* **12**, 829–838 (2009).
12. Bunge, M.B. Novel combination strategies to repair the injured mammalian spinal cord. *J. Spinal Cord Med.* **31**, 262–269 (2008).
13. Ferner, R.E. Neurofibromatosis 1 and neurofibromatosis 2: a twenty first century perspective. *Lancet Neurol.* **6**, 340–351 (2007).
14. Suter, U. & Scherer, S.S. Disease mechanisms in inherited neuropathies. *Nat. Rev. Neurosci.* **4**, 714–726 (2003).
15. Yamaguchi, T. *et al.* Histone deacetylases 1 and 2 act in concert to promote the G1-to-S progression. *Genes Dev.* **24**, 455–469 (2010).
16. Jaegle, M. *et al.* The POU proteins Brn-2 and Oct-6 share important functions in Schwann cell development. *Genes Dev.* **17**, 1380–1391 (2003).
17. Joseph, N.M. *et al.* Neural crest stem cells undergo multilineage differentiation in developing peripheral nerves to generate endoneurial fibroblasts in addition to Schwann cells. *Development* **131**, 5599–5612 (2004).
18. Montgomery, R.L. *et al.* Histone deacetylases 1 and 2 redundantly regulate cardiac morphogenesis, growth, and contractility. *Genes Dev.* **21**, 1790–1802 (2007).
19. Jessen, K.R. & Mirsky, R. The origin and development of glial cells in peripheral nerves. *Nat. Rev. Neurosci.* **6**, 671–682 (2005).
20. Parmantier, E. *et al.* Schwann cell–derived Desert hedgehog controls the development of peripheral nerve sheaths. *Neuron* **23**, 713–724 (1999).
21. Svaren, J. & Meijer, D. The molecular machinery of myelin gene transcription in Schwann cells. *Glia* **56**, 1541–1551 (2008).
22. Zorick, T.S., Syroid, D.E., Brown, A., Gridley, T. & Lemke, G. Krox-20 controls SCIP expression, cell cycle exit and susceptibility to apoptosis in developing myelinating Schwann cells. *Development* **126**, 1397–1406 (1999).
23. Ryu, E.J. *et al.* Misexpression of Pou3f1 results in peripheral nerve hypomyelination and axonal loss. *J. Neurosci.* **27**, 11552–11559 (2007).
24. Jessen, K.R. & Mirsky, R. Negative regulation of myelination: relevance for development, injury, and demyelinating disease. *Glia* **56**, 1552–1565 (2008).
25. Ghislain, J. & Charnay, P. Control of myelination in Schwann cells: a Krox20 cis-regulatory element integrates Oct6, Brn2 and Sox10 activities. *EMBO Rep.* **7**, 52–58 (2006).
26. Zhang, J., Xu, F., Hashimshony, T., Keshet, I. & Cedar, H. Establishment of transcriptional competence in early and late S phase. *Nature* **420**, 198–202 (2002).
27. Werner, T., Hammer, A., Wahlbuhl, M., Bösl, M.R. & Wegner, M. Multiple conserved regulatory elements with overlapping functions determine Sox10 expression in mouse embryogenesis. *Nucleic Acids Res.* **35**, 6526–6538 (2007).
28. LeBlanc, S.E., Jang, S.-W., Ward, R.M., Wrabetz, L. & Svaren, J. Direct regulation of myelin protein zero expression by the Egr2 transactivator. *J. Biol. Chem.* **281**, 5453–5460 (2006).
29. Bordonaro, M., Lazarova, D.L. & Sartorelli, A.C. The activation of beta-catenin by Wnt signaling mediates the effects of histone deacetylase inhibitors. *Exp. Cell Res.* **313**, 1652–1666 (2007).
30. Finzsch, M. *et al.* Sox10 is not only required for Schwann cell specification, but also for maintenance of cell identity and progression beyond the immature Schwann cell stage. *J. Cell Biol.* **189**, 701–712 (2010).
31. Topilko, P. *et al.* Krox-20 controls myelination in the peripheral nervous system. *Nature* **371**, 796–799 (1994).
32. Clevers, H. & van de Wetering, M. TCF/LEF factor earn their wings. *Trends Genet.* **13**, 485–489 (1997).
33. Dutton, J.R. *et al.* An evolutionarily conserved intronic region controls the spatiotemporal expression of the transcription factor Sox10. *BMC Dev. Biol.* **8**, 105–124 (2008).
34. Chen, Y. *et al.* HDAC-mediated deacetylation of NF- $\kappa$ B is critical for Schwann cell myelination. *Nat. Neurosci.* advance online publication, doi:10.1038/nn.2780 (20 March 2011).

## ONLINE METHODS

**Generation of conditional knockout mice.** Mice homozygous for *Hdac1*<sup>loxP/loxP</sup> and/or *Hdac2*<sup>loxP/loxP</sup> 'floxed' alleles<sup>15</sup> were crossed with mice expressing Cre recombinase under control of *Dhh* gene regulatory sequences (*Dhh*<sup>Cre</sup>; ref. 35) to ablate HDAC1 and/or HDAC2 in Schwann cells. Genotypes were determined by PCR on genomic DNA. Animal use was approved by the veterinary office of the Canton of Zurich, Switzerland.

**Electron microscopy.** Processing of mouse sciatic nerves was carried out as previously described<sup>36</sup>.

**Cell culture.** Purified primary RSCs were obtained as described<sup>37</sup> and grown in DMEM containing 10% FCS (Gibco), 1:500 penicillin/streptomycin (Invitrogen), 4  $\mu\text{g ml}^{-1}$  crude glial growth factor (bovine pituitary extract, Biomedical Technologies), and 2  $\mu\text{M}$  forskolin (Sigma), at 37 °C in 5% CO<sub>2</sub>/95% air. For differentiation, RSCs were growth-arrested in defined medium<sup>37</sup> for 8 to 15 h, 1 mM dibutyryl cyclic AMP (dbcAMP; Sigma) was added and cells were incubated in this medium for another 6–7 h (transfection experiments and immunoprecipitations) or 2 d.

**Generation of lentiviruses.** We designed an *Hdac2*-specific shRNA (H2sh), using Dharmacon siDESIGN Center and 2-shRNA Oligo Designer (<http://www.unc.edu/~cail/bioutil/2shRNA.html>). We also generated an *Hdac1*-specific shRNA (H1sh) and a nontargeting shRNA as control. Targeting and nontargeting sequences: H2sh, 5'-GTACTACGCTGTCAACTTT-3'; H1sh, 5'-GCCAGTCATGTCCAAAGTAAT-3'; control, 5'-GCGTTCCTAACTTTGAACC-3' (H1sh and control both Sigma-designed). We cloned the corresponding shRNA oligonucleotides (synthesized by Microsynth) into the pLentiLox 3.7 lentiviral plasmid (ATCC) using either HpaI/XhoI or HpaI/NotI. For the H1sh construct, we replaced GFP by *DsRed2*. pLentiLox 3.7 was digested with EcoRI, blunted, and then digested with NheI. pDsRed2-N1 (Clontech) was digested with NotI, blunted, and then digested with NheI. Excised *DsRed2* was ligated into linearized pLentiLox 3.7. Wnt1- and ABC-overexpressing lentiviral constructs, originally produced by Z. Werb and B. Welm<sup>38</sup> and T. Reya<sup>39</sup>, respectively, were obtained from Addgene (plasmids 18983 and 20673, respectively). pLentiLox expressing *DsRed* or GFP was used as a control for Wnt1 and ABC overexpressions.

To produce lentiviral particles, HEK293T cells were transfected with each lentiviral construct together with the packaging constructs pLP1, pLP2 and pLP/VSVG (Invitrogen) using Lipofectamine 2000 (Invitrogen), according to the recommendations of the manufacturer (ViraPower Lentiviral Expression Systems Manual).

**Transduction of Schwann cells with lentiviruses.** Lentiviruses were incubated for 8–15 h with Schwann cells in culture medium containing 8  $\mu\text{g ml}^{-1}$  Polybrene (Sigma), at a multiplicity of infection of 2–5. Cells were then washed and maintained in culture medium for an additional day when transduced with Wnt1 or ABC-overexpressing lentiviruses, or for another 2 d when transduced with shRNA lentiviruses. Depending on the experiment, cells were either assayed immediately (proliferating conditions) or differentiated before being analyzed.

**Immunofluorescence.** Mouse sciatic nerves were fixed *in situ* with 4% paraformaldehyde (PFA) for 10 min, dissected, embedded in O.C.T. compound (Tissue-Tek), and stored at –80 °C. Rat sciatic nerves were dissected, fixed with PFA for 10 min, washed in PBS, dehydrated in 30% sucrose overnight, embedded in OCT, and stored at –80 °C. Cryosections (5  $\mu\text{m}$  thick) were permeabilized and blocked for 30 min at 20–25 °C in blocking buffer (0.3% Triton X-100 and 10% goat serum in PBS), and incubated with primary antibodies overnight at 4 °C in blocking buffer. Antibodies: ZO-1 and Claudin-1 (both rabbit, 1:500, Zymed), GFAP (mouse, 1:300, Sigma) and S100 (rabbit, 1:200, DakoCytomation; mouse, 1:200, Sigma). To double-stain HDAC1 (rabbit, 1:3,000, Affinity BioReagents) and HDAC2 (mouse, 1:300, Sigma), rat cryosections (5  $\mu\text{m}$  thick) were first incubated in citrate buffer for 2 h at 65 °C. To co-label HDAC2 and S100, or Oct6 (rabbit, 1:300, ref. 40) and apoptotic cells (TUNEL), cryosections were first treated with 100% acetone at –20 °C for 10 min.

Cells were fixed with 4% PFA for 20 min at 4 °C, washed in PBS, blocked for 15 min in blocking buffer, and incubated with primary antibodies (rabbit anti-HDAC1, 1:1,000, Affinity BioReagents; goat anti-HDAC1, 1:200, Santa Cruz

Biotechnology; mouse anti-HDAC2, 1:200, Sigma; rabbit anti-HDAC2, 1:200, Santa Cruz Biotechnology; mouse anti-Sox10, 1:100, R&D Systems; goat anti-Sox10, 1:100, Santa Cruz Biotechnology; rabbit anti-Krox20, 1:200, Covance; mouse anti-ABC, 1:100, Chemicon; rabbit anti-MAG, 1:200, Zymed) overnight at 4 °C in blocking buffer.

In all cases, sections and cells were washed in PBS, incubated with secondary antibodies coupled to Alexa 488 (1:500, Invitrogen), fluorescein isothiocyanate (FITC; 1:500, Jackson ImmunoResearch), Cy3 (1:500, Jackson ImmunoResearch) or Cy5 (1:50, Jackson ImmunoResearch) for 1 h at 20–25 °C, washed in PBS, incubated 5 min with DAPI (to label nuclei), and mounted in Citifluor (Agar Scientific).

Staining was observed using a fluorescence microscope (Axioplan2 Imaging, Carl Zeiss) with 20 $\times$  0.50 numerical aperture, 40 $\times$  0.75 numerical aperture or 63 $\times$  1.25 numerical aperture (oil immersion) Plan Neofluar objectives. Images were digitized with a PowerShot G5 camera (Canon) and acquired with AxioVision 4.5 software (Carl Zeiss). Brightness and contrast of images were adjusted using Adobe Photoshop CS5 Extended version 12.0.1  $\times$  64 (Adobe Systems, Macintosh version).

For confocal analyses, staining was observed using a Leica DMIRE2 inverse microscope and a Leica SP2 AOBs point laser scanning confocal, with a 63 $\times$  1.4 numerical aperture, differential interference contrast, oil immersion, HCX Plan-Apo objective. Optical sections were collected at 0.2  $\mu\text{m}$  intervals using Leica LCS software. Images were assembled, and the brightness and contrast were adjusted using Adobe Photoshop CS5 Extended version 12.0.1  $\times$  64. Single optical sections are shown.

**TUNEL assay.** Longitudinal sciatic nerve sections (7  $\mu\text{m}$  thick) or cells were fixed in 4% PFA for 10 min and blocked for 1 h with 10% goat serum, 2% Triton X-100 and 0.1% BSA in PBS. TUNEL assay was performed according to the manufacturer's instructions (Roche).

**BrdU and EdU (5-ethynyl-2'-deoxyuridine) assays.** BrdU (100 mg per kilogram body weight) was administered to mouse pups by intraperitoneal injection 2 h before death. Longitudinal sciatic nerve sections (7  $\mu\text{m}$  thick) were fixed in 4% PFA for 10 min, washed in PBS and incubated for 15 min at 95 °C in citrate buffer using a microwave histoprocessor. Sections were then washed in PBS and incubated in 0.2% Triton X-100 in PBS for 1 h at 20–25 °C. DNA was denatured by two successive incubation steps of 8 min in 2 N HCl, and the reaction was neutralized by two successive incubations of 8 min in 0.1 M sodium tetraborate, pH 8.5. Sections were then blocked for 2 h at 20–25 °C in blocking buffer (0.2% Triton X-100, 10% goat serum in PBS), and mouse anti-BrdU antibody (1:250, Sigma) was incubated overnight at 4 °C. Sections were then washed in PBS, incubated for 1 h at 20–25 °C with goat anti-mouse–Cy3 antibody (1:500) in blocking buffer, washed again in PBS, and mounted with Citifluor. Nuclei were detected with DAPI and counted on adjacent sections.

For EdU labeling, EdU reagent (Click-iT EdU, Invitrogen) was added to the cells in culture medium and incubated for 1 h at 37 °C and 5% CO<sub>2</sub>/95% air. Cells were then fixed with 4% PFA for 15 min at 20–25 °C and labeled following the recommendations of the manufacturer (Invitrogen).

**Immunoprecipitation and western blotting.** Sciatic nerves were dissected and the perineurium removed. Tissues and cells were lysed and immunoprecipitations carried out as described<sup>37</sup> with modifications: in the lower panel of **Figure 4d**, immunoprecipitating antibodies were cross-linked to Protein A/G PLUS Agarose beads (Santa Cruz Biotechnology) according to the online protocol (<http://www.neb.com/nebecomm/products/protocol52.asp>, New England Biolabs). Proteins were eluted by 0.1 M glycine, pH 2.5, and the eluted material was neutralized by 1 M Tris, pH 8.0. Lysates and immunoprecipitations were subjected to SDS-PAGE and analyzed by western blotting, as described<sup>37</sup>.

**Antibodies for immunoprecipitation and western blotting.** Primary antibodies: rabbit anti-HDAC2 (1:1,000, Santa Cruz Biotechnology), mouse anti-HDAC2 (1:2,000, Sigma), rabbit anti-HDAC1 (1:2,000, Affinity BioReagents), goat anti-HDAC1 (1:1,000, Santa Cruz Biotechnology), rabbit anti-Krox20 (1:500, Covance), mouse anti-Sox10 (1:500, R&D Systems), rabbit anti-P0 (1:2,000, kind gift from D.R. Colman), mouse anti-P0 (1:1,000, ASTEXX), rabbit anti-Oct6 (1:1,000, ref. 40), rabbit anti-MAG (1:1,000, Zymed), rat anti-MBP (1:500, Serotec), mouse anti-ABC (1:500, Chemicon), rabbit anti-Id2 (1:500, Santa Cruz

Biotechnology), rabbit anti-c-Jun (1:1,000, Cell Signaling), rabbit anti-Sox2 (1:5,000, kind gift from M. Wegner), mouse anti-Tcf-4 (1:1,000, Millipore), mouse anti- $\beta$ -actin (1:5,000, Sigma), mouse anti-GAPDH (1:5,000, Hytest).

All secondary antibodies were from Jackson ImmunoResearch. For western blots of sciatic nerves, light chain-specific goat anti-mouse-horseradish peroxidase (HRP) and goat anti-rabbit-HRP and total IgG-specific donkey anti-goat-HRP were used. Two micrograms of antibody were used per immunoprecipitation.

**RT-PCR.** Isolation of mRNA, cDNA reverse transcription, quantitative real-time PCR and primer sequences for *Sox10* and *P0* have been described<sup>41</sup>. Primer sequences for *Krox20* and *Gapdh*: *Krox20*, forward 5'-TTTTTCC ATCTCCGTGCCA-3', reverse 5'-GAACGGCTTTCGATCAGGG-3'; *Gapdh*, forward 5'-GTATCCGTTGTGGATCTGACAT-3', reverse 5'-GCCTGCTCA CCACCTCTTGA-3'.

**Chromatin immunoprecipitation.** Five immunoprecipitations were performed with one confluent 15-cm dish of RSCs. Cells were washed with PBS and cross-linked for 10 min with formaldehyde (1.42%). Glycine (125 mM) was added for 5 min to quench formaldehyde. Samples were then processed using MagnaChip G kit according to the guidelines of the manufacturer (Millipore). Antibodies: rabbit anti-HDAC2, goat anti-HDAC1, mouse anti-HH3 (positive control, Upstate Biotechnology) or rabbit anti-mouse IgG (negative control, Sigma); 2  $\mu$ g were used per immunoprecipitation. Quantitative real-time PCR analyses were performed on a Sequence Detection System (ABI 7000; Applied Biosystems) using the 2 $\times$  SYBR Green PCR Master Mix (Applied Biosystems) according to the manufacturer's recommendations. Amplification program: 10 min at 95 °C, 45 cycles of 15 s at 95 °C, 1 min at 60 °C. A dissociation step was added to verify the specificity of the products formed. Primer sequences: *Krox20* promoter, forward 5'-GGTCGGTGATCGCGCCTTCC-3', reverse 5'-TCGCCCCGAACGATTCGCTG-3'; *Krox20* MSE, forward 5'-GGC ACATGCCGTCCGTGTCA-3', reverse 5'-ATTCTGGACCCGCTCGCAC-3'; *Krox20* exon 2, forward 5'-CCGTAATTTTACTCTTGGGG-3', reverse 5'-CACTGCTGCAGACCCACTG-3'; *Sox10* promoter, forward 5'-AACCCATG CTCCTCTGTTT-3', reverse 5'-CTCTTCTTAGCGAAGGCAGC-3'; *Sox10* intron1, forward 5'-GGGTTCTCCATCTGTCTGA-3', reverse 5'-CATTCC TTTGACGTTAGCC-3'. *P0* promoter, *P0* intron1 and *P0* -2.3-kb primer pairs have been described previously<sup>27</sup>.

**Constructs, transfections and luciferase gene reporter assay.** We generated two mutant constructs from the mammalian expression plasmid named pe1b-Sox10 MCS1C (plasmid 20240, Addgene). In these mutants, the Sox10 binding site ACAA<sup>41</sup> was deleted either completely ( $\Delta$ 155–585) or partially ( $\Delta$ 469–470). To generate pe1b-Sox10 MCS1C  $\Delta$ 155–585, pe1b-Sox10 MCS1C was digested with Pst1, purified on gel and religated. We generated the mutant pe1b-Sox10 MCS1C  $\Delta$ 469–470 by site-directed deletion of pe1b-Sox10 MCS1C, using PicoMax DNA polymerase (Stratagene) and the following primers: forward 5'-GCATGGACA GTTGAAAGGACTGGAGAG-3', reverse 5'-CTCTCCAGTCCTTCAACTG TCCATGC-3'.

Primary RSCs were transfected in defined medium<sup>35</sup> with Fugene 6 (Roche) at a 3:1 ratio (luciferase assay) or 5:1 ratio (western blots and immunofluorescence) of Fugene 6 to DNA. The DNA was incubated in Optimem medium (Invitrogen) for 5 min at 20–25 °C before addition of Fugene 6. The mix of Fugene 6 and DNA was incubated for 25 min at 20–25 °C before being added to the cells.

Eighteen hours after transfection, we added 1 mM dbcAMP. Cells (in six-well dishes) were lysed in 180  $\mu$ l reporter lysis buffer (Promega) 6 h after dbcAMP addition, and assayed for luciferase activity. Twenty microliters of lysate were subjected to two consecutive injections of 25  $\mu$ l luciferase substrate and values were recorded after an integration time of 30 s. Efficiency of transfection was evaluated by measuring  $\beta$ -galactosidase activity of a co-transfected  $\beta$ -galactosidase construct (Promega). RSCs were co-transfected with 2  $\mu$ g luciferase construct (*Sox10* MCS1 (plasmid 20238, Addgene), *Sox10* MCS1C (plasmid 20240, Addgene), *Sox10* MCS1C  $\Delta$ 155–585, *Sox10* MCS1C  $\Delta$ 469–470, *Krox20* promoter (plasmid 21260, Addgene), *Krox20* MSE (plasmid 21261, Addgene), *Krox20* MSE carrying the mutations I, II, VI, VII, VIII, IX and XI<sup>42</sup> (kind gift from M. Wegner), *P0* promoter (plasmid 21259, Addgene), or *P0* intron1 (plasmid 21630, Addgene)), 2  $\mu$ g overexpressing construct (GFP, HDAC1 (kind gift from S. Schreiber), HDAC2 (kind gift from E. Seto) or ABC), and 300 ng  $\beta$ -galactosidase construct. Luciferase activity was normalized to a luciferase-empty control (transfected with the overexpressing construct), and then normalized to  $\beta$ -galactosidase activity. For  $\beta$ -galactosidase activity, we followed the instructions of the manufacturer (Promega). Endogenous  $\beta$ -galactosidase activity (from cells transfected with overexpression construct only) was subtracted. Results are expressed as a percentage of the GFP control value. We verified that no significant change of luciferase activity of the empty luciferase construct pGL3 (Promega, backbone construct of *Krox20* and *P0* luciferase constructs) occurred when GFP, HDAC1, HDAC2, *Sox10* or ABC-overexpressing constructs were co-transfected. Luciferase constructs have been described previously<sup>42–44</sup>.

**Microarray.** Sciatic nerves of P2 *H1/2*<sup>-/-</sup> and control littermate mice were collected, washed in PBS, and frozen in liquid nitrogen after removal of their perineurium. RNA was extracted using RNeasy Lipid Tissue Mini kit (Qiagen), and comparison between *H1/2*<sup>-/-</sup> and control nerves was performed using an Affimetrix GeneChip Mouse Genome 430 2.0 array, in collaboration with the Functional Genomic Center Zurich.

35. Lindeboom, F. *et al.* A tissue-specific knockout reveals that Gata1 is not essential for Sertoli cell function in the mouse. *Nucleic Acids Res.* **31**, 5405–5412 (2003).
36. Pereira, J.A. *et al.* Integrin-linked kinase is required for radial sorting of axons and Schwann cell myelination in the peripheral nervous system. *J. Cell Biol.* **185**, 147–161 (2009).
37. Jacob, C., Grabner, H., Atanasoski, S. & Suter, U. Expression and localization of Ski determine cell type-specific TGF $\beta$  signaling effects on the cell cycle. *J. Cell Biol.* **182**, 519–530 (2008).
38. Welm, B.E., Dijkgraaf, G.J., Bledau, A.S., Welm, A.L. & Werb, Z. Lentiviral transduction of mammary stem cells for analysis of gene function during development and cancer. *Cell Stem Cell* **2**, 90–102 (2008).
39. Barth, A.I., Stewart, D.B. & Nelson, W.J. T cell factor-activated transcription is not sufficient to induce anchorage-independent growth of epithelial cells expressing mutant  $\beta$ -catenin. *Proc. Natl. Acad. Sci. USA* **96**, 4947–4952 (1999).
40. Ghazvini, M. *et al.* A cell type-specific allele of the POU gene Oct-6 reveals Schwann cell autonomous function in nerve development and regeneration. *EMBO J.* **21**, 4612–4620 (2002).
41. Pereira, J.A. *et al.* Dicer in Schwann cells is required for myelination and axonal integrity. *J. Neurosci.* **30**, 6763–6775 (2010).
42. Antonellis, A. *et al.* Identification of neural crest and glial enhancers at the mouse *Sox10* locus through transgenesis in zebrafish. *PLoS Genet.* **4**, e1000174 (2008).
43. Reiprich, S., Kriesch, J., Schreiner, S. & Wegner, M. Activation of *Krox20* gene expression by *Sox10* in myelinating Schwann cells. *J. Neurochem.* **112**, 744–754 (2010).
44. Kao, S.-C. Calcineurin/NFAT signaling is required for neuregulin-regulated Schwann cell differentiation. *Science* **323**, 651–654 (2009).